

# Local Competition and Stochasticity for Adversarial Robustness in Deep Learning

Konstantinos P. Panousis<sup>†</sup> Sotirios Chatzis<sup>†</sup>

Antonios Alexos<sup>‡</sup>

Sergios Theodoridis<sup>§</sup>

<sup>†</sup>Cyprus University of Technology, Limassol, Cyprus

<sup>‡</sup>University of California Irvine, CA, USA

<sup>§</sup>National and Kapodistrian University of Athens, Athens, Greece

[k.panousis@cut.ac.cy](mailto:k.panousis@cut.ac.cy)

## Abstract

This work addresses adversarial robustness in deep learning by considering deep networks with stochastic local winner-takes-all (LWTA) nonlinearities. This type of network units result in sparse representations from each model layer, as the units are organized in blocks where only one unit generates non-zero output. The main operating principle of the introduced units lies on stochastic arguments, as the network performs posterior sampling over competing units to select the winner. We combine these LWTA arguments with tools from the field of Bayesian non-parametrics, specifically the stick-breaking construction of the Indian Buffet Process, to allow for inferring the sub-part of each layer that is essential for modeling the data at hand. Inference for the proposed network is performed by means of stochastic variational Bayes. We perform a thorough experimental evaluation of our model using benchmark datasets, assuming gradient-based adversarial attacks. As we show, our method achieves high robustness to adversarial perturbations, with state-of-the-art performance in powerful white-box attacks.

## 1 Introduction

Despite their widespread success, Deep Neural Networks (DNNs) are notorious for being highly susceptible to adversarial attacks. *Adversarial examples*,

i.e. inputs comprising carefully design perturbations, are designed with the aim of “*fooling*” a considered model into *misclassification*. It has been shown that, even small perturbations in an original input, e.g. an  $L_p$  norm, may successfully render a DNN vulnerable; this highlights the frailness of common DNNs (Papernot et al., 2017). This vulnerability casts serious doubts regarding the safe and confident use of modern DNNs in safety-critical applications, such as autonomous driving (Boloor et al., 2019; Chen et al., 2015), video recognition (Jiang et al., 2019), healthcare (Finlayson et al., 2019) and other real-world scenarios (Kurakin et al., 2016). To address these concerns, significant research effort has been devoted to adversarially-robust DNNs.

Adversarial attacks and associated defense strategies, comprise many different approaches, sharing the same goal; making deep architectures more *reliable* and *robust*. In general, adversarially-robust model are obtained via the following types of strategies: (i) *Adversarial Training*, where a model is trained with both original and perturbed data (Madry et al., 2017; Tramèr et al., 2017; Shrivastava et al., 2017); (ii) *Manifold Projections*, where the original data are projected into a different subspace, presuming that, therein, the effects of the perturbations can be mitigated (Jalal et al., 2017; Shen et al., 2017; Song et al., 2017); (iii) *Stochastic Modeling*, where some randomization of the input data and/or of the neuronal activations of each hidden layer is performed (Prakash et al., 2018; Dhillon et al., 2018; Xie et al., 2017); and (iv) *Preprocessing*, where some aspect of either the data or of the neuronal activations are modified to induce robustness (Buckman et al., 2018; Guo et al., 2017; Kabilan et al., 2018). However, many of the currently considered approaches and architectures are particularly tailored to the specific characteristics of a considered type of attacks. This implies that such a model may fail completely in case the adversarial attack patterns change

in a radical manner. To overcome this challenge, we posit that a paradigm different from common neuronal activation functions, especially ReLU, is needed.

Recently, the DL community has shown fresh interest for more biologically plausible models. In this context, there is an increasing body of evidence from Neuroscience that neurons with similar functions in a biological system are aggregated together in groups, and local competition takes place for their activation (Local-Winner-Takes-All, LWTA, mechanism). Thus, in each block, only one neuron can be active at a given time, while the rest are inhibited to silence. Crucially, it appears that this mechanism is of stochastic nature, in the sense that the same system may produce different activation patterns when presented with exactly the same stimulus at multiple times (Kandel et al., 2000; Andersen et al., 1969; Stefanis, 1969; Douglas and Martin, 2004; Lansner, 2009). Previous instantiations of the LWTA mechanism in deep learning have shown that the obtained sparse representations of the input are quite informative for classification purposes (Lee and Seung, 1999; Olshausen and Field, 1996), while exhibiting *automatic gain control*, *noise suppression* and *robustness to catastrophic forgetting* (Srivastava et al., 2013; Grossberg, 1982; Carpenter and Grossberg, 1988). However, previous authors have not treated them under a systematic stochastic modeling viewpoint, which is a key component in actual biological systems.

Finally, recent works in the community, e.g. Verma and Swami (2019), have explored the susceptibility of the conventional one-hot encoding of the output to adversarial attacks. By borrowing arguments from coding theory, the authors examine the effect of encoding the output using *error-correcting output codes* in the adversarial scenario. The experimental results suggest that such an encoding technique greatly enhances the robustness of a considered architecture while retaining high classification accuracy in the benign context; in addition, it does not require to craft a method explicitly designed to address adversarial attacks with deeply analyzed and taken care of characteristics.

Drawing upon these insights, we propose a new deep network design scheme that is particularly tailored to address adversarially-robust learning. Our approach falls under the stochastic modeling type of approaches. We introduce modeling principles which allow for learning to infer sparse representations of the input at each model layer. In addition, the model is inherently capable of tuning how sparse these representations should be, in a data driven fashion. To this end, we propose a network architecture employing: (i) LWTA nonlinearities; and (ii) an Indian Buffet process (IBP)-based

mechanism for learning which sub-parts of the network are essential for data modeling; this may essentially further nullify a part of the inferred representations, thus further tuning how sparse these representations are. We combine this modeling rationale with Error Correcting Output Codes (Verma and Swami, 2019) to further enhance performance.

We evaluate our approach using well-known benchmark datasets and network architectures<sup>1</sup>. The provided empirical evidence vouch for the potency of our approach, yielding state-of-the-art robustness against powerful white-box-attacks. The remainder of the paper is organized as follows: In Section 2, we introduce the necessary theoretical background. In Section 3, we introduce the proposed approach and describe its rationale and inference algorithms. In Section 4, we perform extensive experimental evaluations, providing insights for the behavior of the produced model. In Section 5, we summarize the contribution of this work, and discuss potential future research directions.

## 2 Technical Background

### 2.1 Indian Buffet Process

The Indian Buffet Process (IBP) (Ghahramani and Griffiths, 2006) defines a probability distribution over infinite binary matrices. IBP can be used as a flexible prior, allowing the number of considered features to be unbounded and inferred in a data-driven fashion. Its construction, ensures sparsity in the obtained representation, while at the same time allowing for more features to emerge, as new observations appear. Here, we focus on the stick-breaking construction of the IBP proposed by Teh et al. (2007), rendering it amenable to Variational Inference. Let us consider  $N$  observations, and a binary matrix  $\mathbf{Z} = [z_{i,k}]_{i,k=1}^{N,K}$ ; each entry therein, indicates the existence of feature  $k$  in observation  $i$ . Taking the infinite limit  $K \rightarrow \infty$ , we can construct the following hierarchical representation (Teh et al., 2007):

$$u_k \sim \text{Beta}(\alpha, 1), \quad \pi_k = \prod_{i=1}^k u_i, \quad z_{j,k} \sim \text{Bernoulli}(\pi_k), \quad \forall j$$

where  $\alpha$  is non-negative parameter, controlling the induced sparsity. In practice,  $K$  is set to be equal to the input dimensionality to avoid the overcomplete feature representation when  $K \rightarrow \infty$ .

---

<sup>1</sup>Supporting implementation is provided at [https://github.com/konpanousis/adversarial\\_ecoc\\_lwta](https://github.com/konpanousis/adversarial_ecoc_lwta).

## 2.2 Local Winner-Takes-All

Let us assume a single layer of an LWTA-based network comprising  $K$  LWTA blocks with  $U$  competing units therein. Each block produces an output  $\mathbf{y}_k$  ( $k = 1, \dots, K$ ), given some input  $\mathbf{x} \in \mathbb{R}^{N \times J}$ . Each linear unit in each block computes its activation  $h_k^u$ ,  $u = 1, \dots, U$ , and the output of the each block is decided via competition. Thus, for each block,  $k$ , and unit,  $u$ , therein, the output reads:

$$y_k^u = g(h_k^1, \dots, h_k^U) \quad (1)$$

where  $g(\cdot)$  is the *competition function*. The activation of each individual neuron follows the conventional inner product computation  $h_k^u = w_{ku}^T \mathbf{x}$ , where  $\mathbf{W} \in \mathbb{R}^{J \times K \times U}$  is the weight matrix of the LWTA layer. In a conventional *hard* LWTA network, the final output reads:

$$y_k^u = \begin{cases} 1, & \text{if } h_k^u \geq h_k^i, \quad \forall i = 1, \dots, U, i \neq u \\ 0, & \text{otherwise} \end{cases} \quad (2)$$

To bypass the restrictive assumption of binary output, more expressive versions of the competition function have been proposed in the literature, e.g., (Srivastava et al., 2013). These generalized *hard* LWTA networks postulate:

$$y_k^u = \begin{cases} h_k^u, & \text{if } h_k^u \geq h_k^i, \quad \forall i = 1, \dots, U, i \neq u \\ 0, & \text{otherwise} \end{cases} \quad (3)$$

This way, only the neuron with the *strongest* activation produces an output in each block, while the others are inhibited to silence, i.e., the zero value. In this way, the output of each layer of the network yields a sparse representation according to the competition outcome within each block. In case of multiple winners the tie can be broken either by index or randomly.

The above schemes do not respect a major aspect that is predominant in biological systems, namely *stochasticity*. We posit that this aspect may be crucial for endowing deep networks with adversarial robustness. To this end, we adopt a scheme similar to Panousis et al. (2019). That work proposed a novel competition function, based on a competitive random sampling procedure. We explain this scheme in detail in the following Section.

## 3 Model Definition

In this work, we consider a principled way of designing deep neural networks in way that renders their inferred representations considerably more robust to adversarial attacks. To this end, we utilize a novel stochastic LWTA type of nonlinearity, and we combine it with

appropriate sparsity-inducing arguments from the nonparametric Bayesian statistics.

Let us assume an input  $\mathbf{X} \in \mathbb{R}^{N \times J}$  with  $N$  examples, comprising  $J$  features each. In conventional deep architectures, each hidden layer comprises nonlinear units; the input is presented to the layer, which then computes an affine transformation via the inner product of the input with weights  $\mathbf{W} \in \mathbb{R}^{J \times K}$ , producing outputs  $\mathbf{Y} \in \mathbb{R}^{N \times K}$ . The described computation for each example  $n$  yields  $\mathbf{y}_n = \sigma(\mathbf{x}_n \mathbf{W} + b) \in \mathbb{R}^K$ ,  $n = 1, \dots, N$ , where  $b \in \mathbb{R}^K$  is a bias factor and  $\sigma(\cdot)$  is a non-linear activation function, e.g. ReLU. An architecture comprises intermediate and output layers.

Under the proposed, stochastic LWTA-based modeling rationale, singular units are replaced by LWTA blocks, each containing a set of competing *linear* units. Thus, the layer input is now presented to each different block and each unit therein, via different weights. Letting  $K$  be the number of LWTA blocks and  $U$  the number of competing units in each block, the weights are now represented via a three-dimensional matrix  $\mathbf{W} \in \mathbb{R}^{J \times K \times U}$ .

Drawing inspiration from Panousis et al. (2019), we postulate that the local competition in each block is performed via a competitive random sampling procedure. The higher the output of a competing unit, the higher the probability of it being the winner. However, the winner is selected stochastically.

In the following, we introduce some discrete latent vectors  $\xi_n \in \text{one\_hot}(U)^K$ , in order to encode the outcome of the local competition between the units in each block. For each data input,  $n$ , the non-zero entry in this one-hot representation denotes the winning unit among the  $U$  competitors in each of the  $K$  blocks of the layer.

To further enhance the stochasticity and regularization of the resulting model, we turn to the nonparametric Bayesian framework. Specifically, we introduce a matrix of latent variables  $Z \in \{0, 1\}^{J \times K}$ , to explicitly regularize the model by inferring whether the model actually needs to use each synaptic weight connection in each layer. Each entry,  $z_{j,k}$ , therein is set to one, if the  $j^{th}$  dimension of the input is presented to the  $k^{th}$  block, otherwise  $z_{j,k} = 0$ . We impose the sparsity-inducing IBP prior over the latent variables  $Z$  and perform inference over them. Essentially, if all the connections leading to some block are set to  $z_{j,k} = 0$ , the block is effectively zeroed-out of the network.

We now define the output of a layer of the considered

model,  $\mathbf{y}_n \in \mathbb{R}^{K \cdot U}$ , as follows:

$$[\mathbf{y}_n]_{ku} = [\boldsymbol{\xi}_n]_{ku} \sum_{j=1}^J (w_{j,k,u} \cdot z_{j,k}) \cdot [\mathbf{x}_n]_j \in \mathbb{R} \quad (4)$$

To facilitate a competitive random sampling procedure in a data-driven fashion, the latent indicators  $\boldsymbol{\xi}_n$  are drawn from a posterior Categorical distribution. The concept is that the higher the output of a linear competing neuron, the higher the probability of it being the winner. We yield:

$$q([\boldsymbol{\xi}_n]_k) = \text{Discrete}\left([\boldsymbol{\xi}_n]_k \middle| \text{softmax}\left(\sum_{j=1}^J [w_{j,k,u}]_{u=1}^U \cdot z_{j,k} \cdot [\mathbf{x}_n]_j\right)\right) \quad (5)$$

The posteriors of the latent variables  $Z$  are drawn from Bernoulli posteriors, such that:

$$q(z_{j,k}) = \text{Bernoulli}(z_{j,k} | \tilde{\pi}_{j,k}) \quad (6)$$

These are trained by means of variational Bayes, as we describe next, while we resort to fixed-point estimation for the weight matrices  $\mathbf{W}$ .

For the output layer of our approach, we perform the standard inner product computation followed by a softmax, while imposing an IBP over the connections, similar to the inner layers.

Specifically, we assume an input  $\mathbf{x} \in \mathbb{R}^{N \times J}$  to a  $C$ -unit output layer with weights  $W \in \mathbb{R}^{J \times C}$ . We introduce an analogous auxiliary matrix of latent variables  $Z \in \{0, 1\}^{J \times C}$ . Thus, the computation for the output  $\mathbf{y} \in \mathbb{R}^{N \times C}$  yields:

$$y_{n,c} = \text{softmax}\left(\sum_{j=1}^J (w_{j,c} \cdot z_{j,c}) \cdot [\mathbf{x}_n]_j\right) \in \mathbb{R} \quad (7)$$

where the posterior latent variables in  $Z$  are drawn independently from a Bernoulli distribution:

$$q(z_{j,c}) = \text{Bernoulli}(z_{j,c} | \tilde{\pi}_{j,c}) \quad (8)$$

To perform variational inference for the model latent variables, we impose a symmetric Discrete prior over the latent indicators,  $[\boldsymbol{\xi}_n]_k \sim \text{Discrete}(1/U)$ . On the other hand, the prior imposed over  $Z$  follows the stick-breaking construction of the IBP, to facilitate data-driven sparsity induction.

The formulation of the proposed modeling approach is now complete. A graphical illustration of the resulting model is depicted in Fig. 1a.

### 3.1 Convolutional Layers

Further, to accommodate architectures comprising convolutional operations, we devise a convolutional

variant inspired from Panousis et al. (2019). Specifically, let us assume an input tensor  $\{\mathbf{X}\}_{n=1}^N \in \mathbb{R}^{H \times L \times C}$  at a specific layer, where  $H, L, C$  are the height, length and channels of the input. We define a set of kernels, each with weights  $\mathbf{W}_k \in \mathbb{R}^{h \times l \times C \times U}$ , where  $h, l, C, U$  are the kernel height, length, channels and competing features maps, and  $k = 1, \dots, K$ . Thus, analogously to the grouping of linear units in the dense layers, in this case, local competition is performed among feature maps. Each kernel is treated as an LWTA block and each layer comprises multiple kernels competing for their outputs. We additionally consider an analogous auxiliary binary matrix  $Z \in \{0, 1\}^K$  to further regularize the convolutional layers.

Thus, at a given layer of the convolutional variant, the output  $\mathbf{Y}_n \in \mathbb{R}^{H \times L \times K \cdot U}$  is obtained via concatenation along the last dimension of the subtensors:

$$[\mathbf{Y}_n]_k = [\boldsymbol{\xi}_n]_k ((z_k \cdot W_k) \star \mathbf{X}_n) \in H \times L \times U \quad (9)$$

where  $\mathbf{X}_n$  is the input tensor for the  $n^{th}$  datapoint, “ $\star$ ” denotes the convolution operation and  $[\boldsymbol{\xi}_n]_k \in \text{one\_hot}(U)$  is a one-hot vector representation with  $U$  components. Turning to the competition function, we follow the same rationale, such that the sampling procedure is driven from the outputs of the competing feature maps:

$$q([\boldsymbol{\xi}_n]_k) = \text{Discrete}\left([\boldsymbol{\xi}_n]_k \middle| \text{softmax}\left(\sum_{h',l'} [(z_k \cdot W_k) \star \mathbf{X}_n]_{h',l',u}\right)\right)$$

We impose an IBP prior on  $Z$ , while the posteriors are drawn from a Bernoulli distribution, such that,  $q(z_k) = \text{Bernoulli}(z_k | \tilde{\pi}_k)$ . We impose an analogous symmetric prior for the latent winner indicators  $[\boldsymbol{\xi}_n]_k \sim \text{Discrete}(1/U)$ . A graphical illustration of the defined layer is depicted in Fig. 1b.

### 3.2 Training & Inference

To train the proposed model, we resort to maximization of the Evidence Lower Bound (ELBO). To facilitate efficiency in the resulting procedures, we adopt the Stochastic Gradient Variational Bayes framework (SGVB) (Kingma and Welling, 2014). However, our model comprises latent variables that are not readily amenable to the reparameterization trick of SGVB, namely, the discrete latent variables  $Z$  and  $\boldsymbol{\xi}$ , and the Beta-distributed stick variables  $\mathbf{u}$ . Thus, we utilize the continuous relaxation based on the Gumbel-Softmax trick (Maddison et al., 2016; Jang et al., 2017) for the Discrete and Bernoulli random variables, as well as the Kumaraswamy distribution-based reparameterization trick (Kumaraswamy, 1980) of the Beta distribution. These are only employed during training.

At inference time, we draw samples from the trained

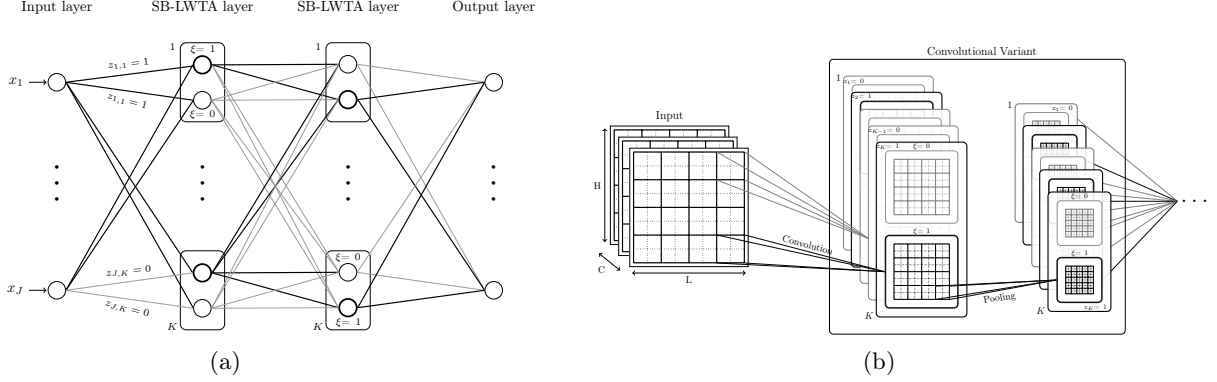


Figure 1: (a) A graphical representation of our competition-based modeling approach. Rectangles denote LWTA blocks, and circles the competing units therein. The winner units are denoted with bold contours ( $\xi = 1$ ). Bold edges denote retained connections ( $z = 1$ ). (b) The convolutional LWTA variant. Competition takes place among feature maps. The winner feature map (denoted with bold contour) passes its output to the next layer, while the rest are zeroed out.

posteriors of the latent variables, i.e. the Discrete and Bernoulli distributions of  $\xi$  and  $z$ ; this introduces stochasticity to the network activations and architecture, respectively. Thus, differently from previous work in the field, the arising stochasticity of the resulting model stems from two different sampling processes. On the one hand, contrary to competition-based networks presented in Srivastava et al. (2013), we implement a data-driven random sampling procedure to determine the winning units. In addition, we infer which subparts of the model must be used or omitted, again based on sampling from the trained posteriors  $q(Z)$ .

## 4 Experimental Evaluation

We evaluate the capacity of our proposed approach against various adversarial attacks and under different setups. To this end, we follow the experimental framework of Verma and Swami (2019). Specifically, we train networks which either employ the standard one-hot representation to encode the output variable of the classifier (predicted class) or an error-correcting output strategy proposed in Verma and Swami (2019); the latter is based on Hadamard coding. We try various activation functions for the classification layer of the networks, and use either a single network or an ensemble, as described in Verma and Swami (2019). The details of the considered networks are provided in Table 1. To obtain some comparative results, the considered networks are formulated under both our modeling approach and in a conventional manner (i.e., with ReLU nonlinearities and SGD training).

Table 1: A summary of the considered networks.  $\mathbf{I}_k$  denotes a  $k \times k$  identity matrix, while  $\mathbf{H}_k$  a  $k$ -length Hadamard code.

Network	Architecture	Code	Output Activation
Softmax	Standard	$\mathbf{I}_{10}$	softmax
Logistic	Standard	$\mathbf{I}_{10}$	logistic
Tanh16	Standard	$\mathbf{H}_{16}$	tanh
LogisticEns10	Ensemble	$\mathbf{I}_{10}$	logistic
TanhEns16	Ensemble	$\mathbf{H}_{16}$	tanh
Madry	Standard	$\mathbf{I}_{10}$	softmax

Table 2: Classification accuracy on MNIST.

Network	Params	Benign	PGD	CW	BSA	Rand	+U(-1, 1)
Softmax (U=4)	327,380	.9613	.865	.970	.950	.187	.729
Softmax (U=2)	327,380	.992	<b>.935</b>	.990	<b>1.0</b>	.961	<b>.838</b>
Logistic (U=2)	327,380	.991	.901	.990	.990	.911	.835
LogEns10 (U=2)	<b>205,190</b>	.993	.889	.980	.970	<b>1.0</b>	.767
Madry	3,274,634	.9853	.925	.84	.520	.351	.150
TanhEns16	401,168	<b>.9948</b>	.929	<b>1.0</b>	<b>1.0</b>	.988	.827

### 4.1 Experimental Setup

We consider two popular benchmark datasets, namely MNIST (LeCun et al., 2010) and CIFAR10 (Krizhevsky, 2009). The networks trained on MNIST are based on the LeNet architecture, while for CIFAR10 we opt for the VGG-like architecture. To evaluate our modeling approach, all the considered networks, depicted in Table 1, are evaluated by splitting the architecture into: (i) LWTA blocks with 2 competing units, and (ii) blocks with 4 competing units. We initialize the posterior parameters of the Kumaraswamy distribution to  $a = K$ ,  $b = 1$ , where  $K$  is the number of LWTA blocks, while using an uninformative Beta prior Beta(1, 1). For the Concrete

relaxations, we set the temperatures of the priors and posteriors to 0.5 and 0.67 respectively, as suggested in Maddison et al. (2016).

Evaluation is performed by utilizing 5 different benchmark adversarial attacks: (i) Projected Gradient Descent (PGD), (ii) Carlini and Wagner (CW), (iii) Blind Spot Attack (BSA) (Zhang et al. (2019)), (iv) a random attack (Rand) Verma and Swami (2019), and (v) an attack comprising additive uniform noise corruption ( $+U(-\gamma, \gamma)$ ). For all attacks, we adopt the exact experimental evaluation of Verma and Swami (2019), both for transparency and comparability.

Specifically, for the PGD attack, we use a common choice for the pixel-wise distortion  $\epsilon = 0.3(0.031)$  for MNIST(CIFAR) with 500(200) attack iterations and a step size of 0.01(0.007). For the CW attack, the learning rate was set to 1e-3 utilizing 10 binary search steps. BSA performs the CW attack with a scaled version of the input  $\alpha x$ ; we set  $\alpha = 0.8$ . In the “Random” attack, we construct random inputs by independently and uniformly generating pixels in  $(0, 1)$  and assess the fraction of which the model’s class probability is less than 0.9. Finally, for the additive uniform noise attack, we set  $\gamma = 1$  for MNIST and  $\gamma = 0.1$  for CIFAR. See the Supplementary Material for the detailed implementation details and experimental setup.

## 4.2 Experimental Results

In the following, we present the comparative experimental evaluation of our approach. We select three out of the five networks of Table 1 to implement our modeling approach with. Then, for brevity, we compare to the best-performing models in Verma and Swami (2019), namely the Madry model (Madry et al., 2017) and the TanhEns16 and TanhEns64 models.

**MNIST.** We train our model for a maximum of 100 epochs, using the same data augmentation as in Verma and Swami (2019). In Table 2, we depict the comparative results for each different network and adversarial attack. As we observe, our modeling approach yields considerable improvements over Madry et al. (2017) and TanhEns16 (Verma and Swami, 2019) in three of the five considered attacks, while imposing lower memory footprint (less trainable parameters). For example, consider the Softmax network formulated with the LWTA blocks of our modeling method, with 2 competing units. In benign classification accuracy, we observe a 0.028% difference in favor of TanhEns16, while the Softmax LWTA model exhibits an improvement of 0.06% in the PGD attack, and 0.011% in the uniform corruption noise attack. This evidence suggests that our approach yields better adversarial robustness, despite the

fact that TanhEns16 requires  $\approx 20\%$  more parameters.

Table 3: Classification accuracy on CIFAR10.

Model	Params	Benign	PGD	CW	BSA	Rand	$+U(-1, 1)$
Tanh16(U=4)	773,600	.5097	.460	.550	.600	.368	.436
Softmax(U=2)	<b>772,628</b>	.8488	<b>.814</b>	<b>.860</b>	<b>.830</b>	.302	.820
Tanh16(U=2)	773,600	.8539	.826	.830	<b>.830</b>	.32	.815
LogEns10(U=2)	1,197,998	.8456	.806	.83	.800	<b>1.0</b>	.812
Madry	45,901,914	.871	.47	.08	0.0	.981	.856
TanhEns64	3,259,456	<b>.896</b>	.601	.760	.760	<b>1.0</b>	<b>.875</b>

**CIFAR-10.** For the CIFAR-10 dataset, we follow an analogous procedure. The obtained comparative effectiveness of our approach is depicted in Table 3. In this case, the differences in the computational burden are more evident, since now the trained networks are based on the VGG-like architecture. As in the previous experiments, our method presents significant improvements in three of the considered adversarial attacks, namely PGD, CW and BSA, while requiring *significantly less parameters* (even 2 to 4 times) than the best performing alternative of Verma and Swami (2019).

## 4.3 Further Insights

### 4.3.1 Ablation Study

To assess the individual utility of LWTA-winner and architecture sampling, we examine the recognition performance and the robustness in both the benign case, as well as in the considered adversarial attacks. Specifically, we consider two different settings: (i) utilizing only the LWTA mechanism in place of conventional ReLU activations, (ii) combining LWTA and IBP. The comparative results can be found in Tables 4 (MNIST) and 5 (CIFAR). Therein, baseline corresponds to the accuracies reported in Verma and Swami (2019).

Thus, we initially study the impact of the LWTA mechanism, and how this mechanism affects the robustness of a considered architecture. To this end, we replace the activations in the architectures of Verma and Swami (2019) with LWTA blocks of competing units. We begin with the MNIST dataset, where we examine two additional setups. Specifically, we employ the deterministic LWTA competition function as defined in (3) and examine its effect against adversarial attacks, both as a standalone modification (denoted as  $LWTA^{max}$ ) and also combined with the IBP prior. The resulting classification performance is illustrated in the second and third row for each network in Table 4. One can observe that using LWTA activations, even without stochastically sampling the winner, yields some improvement, which becomes more prominent with the incorporation of the IBP prior.

The fourth and fifth rows correspond to the *proposed*

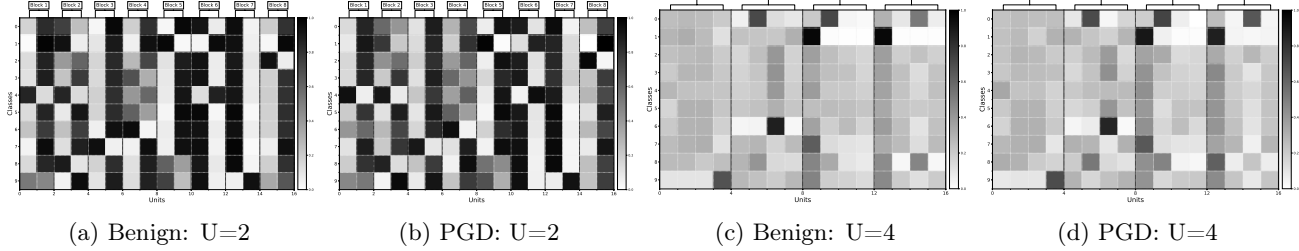


Figure 2: Probabilities of competing units in LWTA blocks, of an intermediate layer of the Tanh16 model, for each class in the CIFAR-10 dataset. Figs. 2a and 2b depict the activations of a model layer with 2 competing units, for benign and PGD test examples, respectively. Figs. 2c and 2d correspond to a network layer comprising 4 competing units. Black denotes very high winning probability, while white denotes very low probability.

Table 4: Classification accuracy for all the attacks on the MNIST dataset.

Model	Method	Benign	PGD	CW	BSA	RAND	Uniform
Softmax	Baseline	.9918	.082	.540	.180	.270	.785
	LWTA <sup>max</sup>	.993	.302	.800	.390	.543	.671
	LWTA <sup>max</sup> & IBP	<b>.994</b>	.890	.920	.840	.361	.717
	LWTA	.992	.900	<b>.990</b>	<b>1.0</b>	.810	.708
Logistic	LWTA & IBP	.992	<b>.935</b>	<b>.990</b>	<b>1.0</b>	<b>.961</b>	<b>.838</b>
	Baseline	.9933	.093	.660	.210	.684	.829
	LWTA <sup>max</sup>	.9933	.388	.780	.420	.700	.718
	LWTA <sup>max</sup> & IBP	<b>.9934</b>	.894	.960	.950	.230	.658
LogisticEns10	LWTA	.991	.856	<b>.990</b>	<b>.990</b>	<b>.982</b>	.802
	LWTA & IBP	.991	<b>.901</b>	<b>.990</b>	<b>.990</b>	.911	<b>.835</b>
	Baseline	.9932	.382	.880	.480	.905	<b>.812</b>
	LWTA <sup>max</sup>	.9934	.303	.920	.520	.900	.754
Tanh16	LWTA <sup>max</sup> & IBP	<b>.9938</b>	.860	.940	.910	.400	.672
	LWTA	.992	.603	.900	.550	.809	.787
	LWTA & IBP	.993	<b>.889</b>	<b>.980</b>	<b>.970</b>	<b>1.0</b>	.767
	Baseline	.9931	.421	.790	.320	.673	.798
Tanh16	LWTA <sup>max</sup>	.992	.462	.910	.420	.573	.674
	LWTA <sup>max</sup> & IBP	<b>.9939</b>	.898	.960	.940	.363	.683
	LWTA	.992	.862	<b>.990</b>	<b>.980</b>	<b>.785</b>	.733
	LWTA & IBP	.990	<b>.900</b>	.980	<b>.980</b>	.775	<b>.810</b>

LWTA stochastic activations, described in the previous section. The experimental results suggest that the stochastic nature of the proposed activation significantly contributes to the robustness of the model; it yields significant gains in all adversarial attacks compared to both the baseline, as well as to the deterministic LWTA adaptation. Finally, stochastic architecture sampling via the IBP-induced mechanism increases even more the robustness of the trained models.

The corresponding experimental results for the CIFAR datasets are provided in Table 5. The empirical evidence vouches for the merits of our approach, which exhibits a significant increase in the capacity of the networks to defend against various adversarial attacks.

#### 4.4 LWTA Behavior

Here, we scrutinize the competition patterns resulting from the employed LWTA mechanism, in order to gain some further insights. First and foremost, we want to ensure that competition does not collapse to singu-

Table 5: Classification accuracy for all the attacks on the CIFAR dataset.

Model	Method	Benign	PGD	CW	BSA	RAND	Uniform
Softmax	Baseline	<b>.864</b>	.070	.080	.040	.404	.815
	LWTA	.8452	.804	.82	<b>.87</b>	<b>.701</b>	.803
	LWTA + IBP	.8488	<b>.814</b>	<b>.86</b>	.83	.302	<b>.820</b>
Logistic	Baseline	<b>.865</b>	.006	.140	.100	.492	<b>.839</b>
	LWTA	.720	.701	.720	.696	.690	.700
	LWTA + IBP	.7471	<b>.738</b>	<b>.800</b>	<b>.820</b>	<b>.726</b>	.721
LogisticEns10	Baseline	<b>.877</b>	.100	.240	.140	.495	<b>.852</b>
	LWTA	.8671	.712	.750	.750	.803	.795
	LWTA + IBP	.8456	<b>.806</b>	<b>.830</b>	<b>.800</b>	<b>1.0</b>	.812
Tanh16	Baseline	<b>.866</b>	.099	.080	.100	.700	<b>.832</b>
	LWTA	.751	.720	.750	.750	<b>.800</b>	.712
	LWTA + IBP	.8539	<b>.826</b>	<b>.830</b>	<b>.830</b>	.320	.815

lar ‘‘always-winning’’ units. To this end, we choose a random intermediate layer of a Tanh16 network formulated under our modeling approach. We consider layers comprising 8 or 4 LWTA blocks of 2 and 4 competing units, respectively, and focus on the CIFAR-10 dataset. The probabilities of unit activations for each class are depicted in Fig. 2. As we observe, the unit activation probabilities for each different setup (benign and PGD) are essentially the same. This suggests that the LWTA mechanism succeeds in encoding salient discriminative patterns in the data that are resilient to PGD attacks. This empirical evidence suggests that we can obtain networks able to defend against adversarial attacks in a principled way; our reported performance results do corroborate this claim.

Further, in Figs. 2c and 2d we depict the corresponding probabilities when employing 4 competing units. In this case, the competition mechanism is uncertain about the winning unit in each block and for each class; average activation probability for each unit is around  $\approx 50\%$ . Moreover, there are several differences in the activations between the benign data and a PGD attack; these explain the significant drop in performance. This behavior potentially arises due to the relatively small structure of the network; from the 16 units of the original architecture, only 4 are active for each input. Thus,

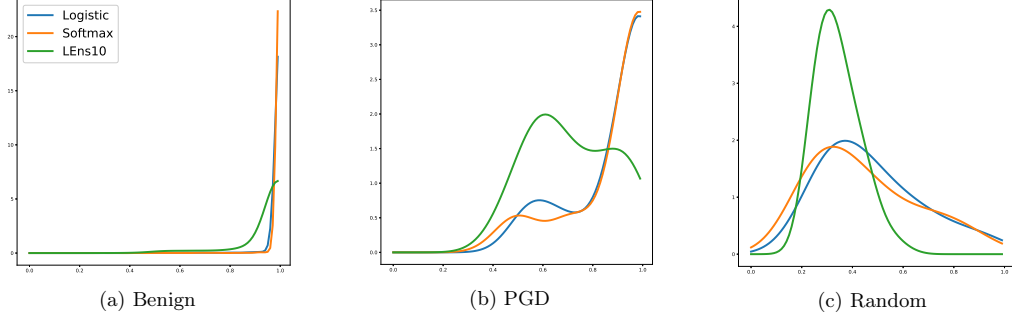


Figure 3: Probability estimates assigned to the most probable class on the test-set of MNIST.

in this setting, LWTA fails to encode the necessary distinctive patterns of the data. Analogous illustrations for different setups are provided in the Supplementary.

Then, we examine the uncertainty estimation capabilities of the introduced approach via the resulting confidence in the classification task. To this end, and similar to Verma and Swami (2019), we compare the probability distributions of class assignment over a randomly chosen set of test examples of the MNIST dataset for our best performing models, with  $U = 2$ . Since our approach yields high classification accuracy in the benign case, we expect that it should exhibit high confidence in label assignment. We depict the expected behavior in Fig. 3a. Fig. 3b depicts the behavior on a PGD attack. We observe that in some cases our model is (correctly) less confident about the class label due to the adversarial perturbations. However, and contrary to Verma and Swami (2019); Madry et al. (2017), the model assigns substantial probability mass in high confidence levels; this results in retaining high classification accuracy. This empirical evidence suggests that by employing a careful blend of LWTA activations and the IBP-induced mechanism, we can overcome the “irrational” overconfidence of the softmax activation. Softmax *incorrectly* assigns high confidence to the class with the largest logits, even in the presence of adversarial examples. Thus, we can overcome this flaw, even when employing small length error correcting output codes. Finally, Fig. 3c illustrates the resulting behavior in randomly generated inputs. In this case, all models correctly place most of the probability mass in the low spectrum, vouching for the success of our approach against various attacks. The corresponding CIFAR-10 graphs can be found in the Supplementary.

## 5 Conclusions

This work aimed to create networks that exhibit more robust and reliable behavior to adversarial attacks. To this end, we utilized local competition be-

tween linear units, in the form of a sampling-based Local-Winner-Takes-All mechanism, combined with a sparsity-inducing IBP prior in order to enhance the stochasticity of the model. Our experimental evaluations have provided strong empirical evidence for the efficacy of our approach. The proposed method exhibits considerable improvements in various kinds of adversarial attacks, while retaining high accuracy in the benign context. It is noteworthy that the competition mechanism yielded very similar competition patterns for benign and adversarial examples. This suggests that the considered approach succeeds in encoding differentially essential sub-distributions of the data through specialization.

## References

Andersen, P., Gross, G. N., Lomo, T., and Sveen, O. (1969). Participation of inhibitory and excitatory interneurones in the control of hippocampal cortical output. In *UCLA forum in medical sciences*, volume 11, page 415.

Boloor, A., He, X., Gill, C., Vorobeychik, Y., and Zhang, X. (2019). Simple physical adversarial examples against end-to-end autonomous driving models. In *2019 IEEE International Conference on Embedded Software and Systems (ICESS)*, pages 1–7. IEEE.

Buckman, J., Roy, A., Raffel, C., and Goodfellow, I. J. (2018). Thermometer encoding: One hot way to resist adversarial examples. In *ICLR*.

Carpenter, G. A. and Grossberg, S. (1988). The art of adaptive pattern recognition by a self-organizing neural network. *Computer*, 21(3):77–88.

Chen, C., Seff, A., Kornhauser, A., and Xiao, J. (2015). Deepdriving: Learning affordance for direct perception in autonomous driving. In *Proceedings of the IEEE International Conference on Computer Vision*, pages 2722–2730.

Dhillon, G. S., Azizzadenesheli, K., Lipton, Z. C., Bernstein, J., Kossaifi, J., Khanna, A., and Anand-

kumar, A. (2018). Stochastic activation pruning for robust adversarial defense. *arXiv preprint arXiv:1803.01442*.

Douglas, R. J. and Martin, K. A. (2004). Neuronal circuits of the neocortex. *Annu. Rev. Neurosci.*, 27:419–451.

Finlayson, S. G., Bowers, J. D., Ito, J., Zittrain, J. L., Beam, A. L., and Kohane, I. S. (2019). Adversarial attacks on medical machine learning. *Science*, 363(6433):1287–1289.

Ghahramani, Z. and Griffiths, T. L. (2006). Infinite latent feature models and the indian buffet process. In *Advances in neural information processing systems*, pages 475–482.

Grossberg, S. (1982). Contour enhancement, short term memory, and constancies in reverberating neural networks. In *Studies of mind and brain*, pages 332–378. Springer.

Guo, C., Rana, M., Cisse, M., and Van Der Maaten, L. (2017). Countering adversarial images using input transformations. *arXiv preprint arXiv:1711.00117*.

Jalal, A., Ilyas, A., Daskalakis, C., and Dimakis, A. G. (2017). The robust manifold defense: Adversarial training using generative models. *arXiv preprint arXiv:1712.09196*.

Jang, E., Gu, S., and Poole, B. (2017). Categorical reparametrization with gumbel-softmax. In *Proceedings International Conference on Learning Representations 2017*.

Jiang, L., Ma, X., Chen, S., Bailey, J., and Jiang, Y.-G. (2019). Black-box adversarial attacks on video recognition models. In *Proceedings of the 27th ACM International Conference on Multimedia*, pages 864–872.

Kabilan, V. M., Morris, B., and Nguyen, A. (2018). Vectordefense: Vectorization as a defense to adversarial examples. *arXiv preprint arXiv:1804.08529*.

Kandel, E. R., Schwartz, J. H., Jessell, T. M., of Biochemistry, D., Jessell, M. B. T., Siegelbaum, S., and Hudspeth, A. (2000). *Principles of neural science*, volume 4. McGraw-hill New York.

Kingma, D. P. and Welling, M. (2014). Auto-encoding variational bayes. In Bengio, Y. and LeCun, Y., editors, *ICLR*.

Krizhevsky, A. (2009). Learning multiple layers of features from tiny images. Technical report.

Kumaraswamy, P. (1980). A generalized probability density function for double-bounded random processes. *Journal of Hydrology*, 46(1):79 – 88.

Kurakin, A., Goodfellow, I., and Bengio, S. (2016). Adversarial examples in the physical world. *arXiv preprint arXiv:1607.02533*.

Lansner, A. (2009). Associative memory models: from the cell-assembly theory to biophysically detailed cortex simulations. *Trends in neurosciences*, 32(3):178–186.

LeCun, Y., Cortes, C., and Burges, C. (2010). Mnist handwritten digit database. *ATT Labs [Online]. Available: <http://yann.lecun.com/exdb/mnist>*, 2.

Lee, D. D. and Seung, H. S. (1999). Learning the parts of objects by non-negative matrix factorization. *Nature*, 401(6755):788–791.

Maddison, C. J., Mnih, A., and Teh, Y. W. (2016). The concrete distribution: A continuous relaxation of discrete random variables. *arXiv preprint arXiv:1611.00712*.

Madry, A., Makelov, A., Schmidt, L., Tsipras, D., and Vladu, A. (2017). Towards deep learning models resistant to adversarial attacks. *arXiv preprint arXiv:1706.06083*.

Olshausen, B. A. and Field, D. J. (1996). Emergence of simple-cell receptive field properties by learning a sparse code for natural images. *Nature*, 381(6583):607–609.

Panousis, K., Chatzis, S., and Theodoridis, S. (2019). Nonparametric Bayesian deep networks with local competition. In Chaudhuri, K. and Salakhutdinov, R., editors, *Proceedings of the 36th International Conference on Machine Learning*, volume 97 of *Proceedings of Machine Learning Research*, pages 4980–4988, Long Beach, California, USA. PMLR.

Papernot, N., McDaniel, P., Goodfellow, I., Jha, S., Celik, Z. B., and Swami, A. (2017). Practical black-box attacks against machine learning. In *Proceedings of the 2017 ACM on Asia conference on computer and communications security*, pages 506–519.

Prakash, A., Moran, N., Garber, S., DiLillo, A., and Storer, J. (2018). Deflecting adversarial attacks with pixel deflection. In *Proceedings of the IEEE conference on computer vision and pattern recognition*, pages 8571–8580.

Shen, S., Jin, G., Gao, K., and Zhang, Y. (2017). Apegan: Adversarial perturbation elimination with gan. *arXiv preprint arXiv:1707.05474*.

Shrivastava, A., Pfister, T., Tuzel, O., Susskind, J., Wang, W., and Webb, R. (2017). Learning from simulated and unsupervised images through adversarial training. In *Proceedings of the IEEE conference on computer vision and pattern recognition*, pages 2107–2116.

Song, Y., Kim, T., Nowozin, S., Ermon, S., and Kushman, N. (2017). Pixeldefend: Leveraging generative models to understand and defend against adversarial examples. *arXiv preprint arXiv:1710.10766*.

Srivastava, R. K., Masci, J., Kazerounian, S., Gomez, F., and Schmidhuber, J. (2013). Compete to compute. In *Advances in neural information processing systems*, pages 2310–2318.

Stefanis, C. (1969). Interneuronal mechanisms in the cortex. In *UCLA forum in medical sciences*, volume 11, page 497.

Teh, Y. W., Grür, D., and Ghahramani, Z. (2007). Stick-breaking construction for the indian buffet process. In *Artificial Intelligence and Statistics*, pages 556–563.

Tramèr, F., Kurakin, A., Papernot, N., Goodfellow, I., Boneh, D., and McDaniel, P. (2017). Ensemble adversarial training: Attacks and defenses. *arXiv preprint arXiv:1705.07204*.

Verma, G. and Swami, A. (2019). Error correcting output codes improve probability estimation and adversarial robustness of deep neural networks. In *Advances in Neural Information Processing Systems*, pages 8643–8653.

Xie, C., Wang, J., Zhang, Z., Ren, Z., and Yuille, A. (2017). Mitigating adversarial effects through randomization. *arXiv preprint arXiv:1711.01991*.

Zhang, H., Chen, H., Song, Z., Boning, D., Dhillon, I. S., and Hsieh, C.-J. (2019). The limitations of adversarial training and the blind-spot attack. *arXiv preprint arXiv:1901.04684*.